

Impacts of Zn and Cu enrichment under ocean acidification scenario on a phytoplankton community from tropical upwelling system

Diksha Sharma^{1*}, Haimanti Biswas¹, Saumya Silori¹, D. Bandyopadhyay^{1,2}, Aziz urRahman Shaik¹, Damien Cardinal³, Magloire Mandeng-Yogo⁴ and Durbar Ray¹.

¹CSIR National Institute of Oceanography, Biological Oceanography Division,
Dona Paula, Goa 403 004, India

*Affiliated for PhD under Bharathidasan University, Tiruchirappalli, TN 620024, India.

² Present address: National Center for Coastal Research, (ICMAM-PD) NIOT Campus, Velachery,
Tambaram Main Rd, Pallikaranai, Chennai, Tamil Nadu 600100.

³Laboratoire d'Océanographie et du Climat: Expérimentations et Approches Numériques (LOCEAN UMR7159, SU, IRD,
CNRS, MNHN), Sorbonne Université, 4 Place Jussieu, 75005 Paris, France

⁴LOCEAN (UMR7159, SU, IRD, CNRS, MNHN) - Institut de recherche pour le développement (IRD),
32 Avenue Henri Varagnat, 93140 Bondy, France

Corresponding author's telephone and email: +91 (832) 2450 280; haimanti.biswas@nio.org

Abstract

Increasing dissolution of CO₂ in the surface ocean is rapidly decreasing its pH and changing carbon chemistry which is further affecting marine biota in several ways. Phytoplankton response studies under the combination of elevated CO₂ and trace metals are rare. We have conducted two consecutive onboard incubation experiments (*R. V. Sindhu Sadhana*; August 2017) in the eastern Arabian Sea (SW coast of India) during an upwelling event. A nutrient enriched diatom bloom was initiated onboard and grown under ambient ($\approx 400 \mu\text{atm}$, A-CO₂) and high CO₂ levels ($\approx 1000 \mu\text{atm}$; H-CO₂) with different zinc (Zn; 1nM) and copper (Cu) concentrations (1nM, 2nM and 8nM). Phytoplankton community composition and the dominant genera were different during these two experiments. CO₂ enrichment alone did not show any significant growth stimulating impact on the experimental community except enhanced cell density in the first experiment. Addition of Zn at A-CO₂ level revealed no noticeable responses; whereas, the same treatment under H-CO₂ level significantly reduced cell number. Considerably high protein content under H-CO₂+Zn treatment was possibly counteracting Zn toxicity which also caused slower growth rate. Cu addition did not show any noticeable impact on growth and biomass production except increased protein content as well as decreased carbohydrate: protein ratio. This can be attributed to relatively higher protein synthesis than carbohydrate to alleviate oxidative stress generated by Cu. The centric diatom *Chaetoceros* and toxin producing pennate diatom *Pseudo-nitzschias* showed no significant response to either CO₂ or Zn enrichment. Large centric diatom *Leptocylindrus* and *Skeletonema* responded positively to Zn addition in both CO₂ levels. The former species showed the most sensitive response at the highest Cu and H-CO₂ treatment; whereas, the pennate diatoms *Nitzschia* and *Pseudo-nitzschia* (toxigenic diatom) showed higher resilience under elevated CO₂ and Cu levels. This observation indicated that in future ocean, increasing CO₂ concentrations and trace metal pollution may potentially alter phytoplankton community structure and may facilitate toxigenic diatom bloom in the coastal waters.

Key words: Arabian Sea; Upwelling; Ocean acidification; Copper; Zinc; Phytoplankton, Diatoms

Introduction

Since the beginning of the industrial revolution, atmospheric CO₂ concentration is rising steadily as a result of decreasing sinks and increasing sources of CO₂ mostly due to human activities. According to IPCC (2013) atmospheric CO₂ level is likely to double by the end this century. Approximately, 25% of atmospheric CO₂ emitted every year by anthropogenic activities is absorbed by the oceans (De Vries, 2014; De Vries et al., 2017). Increasing dissolution of CO₂ in the surface ocean is leading to a rapid decrease in pH (increase in H⁺ ion concentrations) and other related changes in carbon chemistry (increasing CO₂ and HCO₃⁻ and decreasing CO₃²⁻ concentrations). These changes in inorganic carbon speciation and increase in H⁺ ion concentration are further affecting marine biota in various ways. The shift of pH toward less alkaline conditions is referred to Ocean Acidification (OA). The surface seawater pH has already dropped by 0.1 unit from its pre-industrial value (Feely et al., 2004) and is predicted to decrease further (Hester et al., 2008). Most of the biogeochemical processes occurring in the marine environments are sensitive to pH changes, since pH is a key factor that mediates chemical and physiological processes. OA is imposing a serious threat to the marine organisms by altering its diversity on a global scale (Kroeker et al., 2013a) and such threats are further intensifying in some parts of the world oceans, mostly due to regional processes (physical, chemical and biological) (Hurd et al., 2018).

Marine phytoplankton, the base of the marine trophic network, can be highly sensitive to OA (Bach et al., 2017; Pardew et al. 2018; Riebesell, 2004). In general, it is difficult for marine phytoplankton to accumulate sufficient Dissolved Inorganic Carbon (DIC) inside the cell to run photosynthesis at an optimal rate due to 1) very low concentrations of dissolved CO₂ (<1% of DIC) in the surface seawater and 2) extremely low affinity of RubisCO, the main carboxylating enzyme, towards CO₂ (Falkowski and Raven, 2007). Hence, the projected CO₂ level may be beneficial for marine phytoplankton in terms of DIC transport and photosynthesis (Reinfelder, 2011); however, low pH may alter their respiration and net carbon accumulation rates as well as other biochemical reactions (Spilling et al. 2016).

The rate of OA in the open ocean regions can be significantly different than in the coastal seas due to higher dynamicity of the latter (Chan et al., 2017). Our earlier experiments showed that the coastal diatom community from the both Bay of Bengal (BoB) and Arabian Sea (AS) responded positively to CO₂ enrichment (Biswas et al., 2017; Shaik et al., 2017). The organisms living in the polluted coastal waters and upwelling regions where the concentrations of dissolved CO₂ levels are usually naturally higher, are likely to be well adapted to a wide range of pH (Brown et al., 2018;

Bracken et al. 2018). The biological response studies in such natural environments are extremely important in order to develop a mechanistic understanding about living in a high CO₂ world.

Global ocean is not only facing the problem of OA, but other stressors (e. g. temperature, light, dissolved oxygen, trace metals) are also changing simultaneously. The combined effects of OA along with the other variables bear considerable capacity to impact ecosystem functioning rather than OA alone (Haigh et al., 2015) and marine phytoplankton showed high level of diverse and complex responses (Boyd and Hutchins, 2012; Boyd et al., 2018; Gao et al., 2017; Keyset al., 2018; Taucher et al., 2018). Hence, understanding the biological response to such multifaceted changes is of high research priority (Boyd, 2018; Kroeker et al., 2013) for policy making and ocean management (Hurd et al., 2018).

Dissolved trace metals like, iron (Fe), copper (Cu) and zinc (Zn) are crucial for marine phytoplankton growth and the changing H⁺ concentration in the upper ocean may significantly impact trace metal chemistry, metal uptake rates (Shi et al. , 2010), their bioavailability and toxicity (Leal et al., 2018; Millero et al., 2009). Understanding trace metal chemistry under OA scenario is an emerging field of study (Millero et al., 2009; Stockdale et al. 2016). Trace metals present in the marine environment usually form strong and weak complexes with different organic ligands; the concentrations of free metal ions can be very small (<1%) relative to the organically bound complexes (>99%) (Sunda and Huntsman, 1998). In general, there is a competition between H⁺ and metal ions to be attached to the active sites of organic ligands. With increase of H⁺ concentrations, the active sites of the organic ligands are occupied by H⁺ ions via release of free metal ions. Likewise, Stockdale et al. (2016) calculated the availability of free metal ions using a chemical speciation model under IPCC scenario 4 (considering peak emission) and revealed a 1.5 times increase in free Cu ions by the year 2100. The second factor that may reduce trace metal availability is less amount of weak metal ion complex formation under high H⁺ concentrations (Xu et al. 2012).

Coastal waters receive significant amount of trace metals from different anthropogenic sources like antifouling paints, industrial and transport pollution (Nriagu, 1989). In general trace metals like Cu can negatively impact marine phytoplankton growth (Lopez et al. 2019) above a certain level. However, some phytoplankton species may have special physiological mechanisms to grow under toxic Cu levels. For instance, Cu toxicity varied linearly with increasing distance from the coast in the BoB, indicating higher resilience of the coastal phytoplankton under Cu stress than the offshore offspring (Biswas and Bandyopadhyay, 2017). Recently, the co-occurrence of Cu pollution and harmful algal bloom was observed in the coastal waters (Wells et al. 2015). Similarly, Paytan et al. (2009) have shown that urban aerosols could be a potential source of Cu causing toxic

effects on marine phytoplankton. Moreover, coastal waters in the southwest coast of India get naturally CO₂ enriched due to SW monsoon induced upwelling and Rejomon et al. (2009) reported quite high values of dissolved Zn (15±4.9nM) and Cu (21±5.6nM) in the offshore and shelf waters from this region which also receives substantial amount of urban aerosol (Kalapureddy et al., 2009). Such aerosols can have high anthropogenic Zn and Cu enrichment as reported by Gaonkar et al. (2019) in the atmospheric particulate matter collected over a coastal city next to the eastern AS. Hence, natural CO₂ enrichment and addition of trace metals in the western Indian shelf waters may collectively impact phytoplankton growth. The experimental evidences on the responses of marine phytoplankton to such combined stressors are rare from this area. The present study was undertaken 1) to assess the impacts of increasing CO₂ supply and 2) to understand the combined impacts of increasing CO₂ as well as Zn and Cu addition on the growth, physiology and community composition of a phytoplankton population from AS upwelling region. .

Material and methods:

Onboard water sample collection and phytoplankton stock culture development:

Two consecutive experiments (Exp I and Exp II) were conducted onboard [RV Sindhu Sadhana (SSD 40)] during the SW monsoon (August 3 -31, 2017). Exp I was carried out to assess the impact CO₂+Zn enrichment and Exp II addressed the effects of CO₂+Cu on the experimental phytoplankton community. All bottles (transparent polycarbonate, Nalgene, USA) used in this experiment were washed with 10% HCl followed by repeated MQ (Millipore) wash and were kept tightly closed inside the individual zip lock bags.

Surface seawater (2m depth) was collected from a coastal station (10.52°N, 75.16°E; Fig. 1a) by using a NISKIN water samplers attached to a CTD-rosette and transferred to acid (10% HCl) cleaned polycarbonate bottles (Nalgene, USA). For analyzing background trace metal concentrations, immediately after collection, the seawater samples were filtered (Polycarbonate membrane Millipore, 0.45µm, 47mm) followed by acidification (ultra-pure HNO₃ pH <2.0). In laboratory (NIO, Goa), the acidified seawater samples were diluted (100 times) with extra-pure water and the dissolved trace concentrations measured without matrix separation with High Resolution ICP-MS (Model: *Nu instrument Attom ES*) equipped with micro-nebulizer (Rodushkin and Ruth, 1997) using ¹⁰³Rhsolution as internal standard. International Certified Reference Material SLEW-3 (estuarine water from NRC, Ottawa, Canada) was used to check the accuracy of the method and showed a good agreement with the certified values (within 95% confidence; precision>5.0%).

The bulk (90L) seawater (filled in clean bottles) was kept inside a dark temperature-controlled room (4°C) until used. This water was filtered through GF/F (Advantec, Japan) filters to remove all biomass and collected into eight (9L) bottles for the main experiments. The intention of removing the initial biomass was to monitor the particulate organic carbon (POC) development without any interference of the existing POC (alternative of synthetic seawater). This also removes the degradation effect of the heterotrophic bacteria which may perturb the DIC system. The same practice has also been adapted for our earlier experimental work from Indian coastal waters (Biswas et al. 2017; Shaik et al. 2017). The natural trace metals concentrations also allow mimicking the natural environment more accurately. It is important to note that for these experiments, the natural phytoplankton community has been modified. Indeed, in order to avoid the impact of natural grazers inside the experimental bottle, an artificial bloom was initiated onboard under the manipulated conditions. We noticed during our earlier experiments that any trace metal enrichment may lead to decreasing grazer and higher phytoplankton biomass accumulation (Biswas and Bandyopadhyay, 2017). Such trend cannot be attributed to growth-stimulating impact and would shadow the real impact of metals on phytoplankton physiology that we want to focus on here.

In order to initiate a mixed phytoplankton bloom, the natural seawater sample was concentrated on a polycarbonate membrane filter (2µm, 47mm, Millipore) without applying any pressure. This concentrated mass was mixed with some ambient seawater and kept in a clean bottle. The initial nutrient concentrations were measured and found to be quite low (DIP <0.5µM; DSi and nitrate+nitrite<2µM). Simultaneously, 5L water was filtered (GF/F, Advantec Japan) using an acid cleaned glass filtration unit inside a clean bench and supplemented with nitrate (NO₃), silicate (Si(OH)₄; DSi) and phosphate (PO₄; DIP) (Table 1). This water was uniformly distributed into two 2L bottles. The concentrated biomass was used as inoculums and was added (10ml) to each bottle. These bottles were kept closed inside a water bath under natural day-night cycle for phytoplankton growth on deck. The light intensity was manipulated by using a black nylon mesh to mimic the light intensity reaching at 2m depth (Fig. 1b). A Lux-meter was used to measure sunlight variability on hourly basis (Fig. 1b) and was converted to µmol Einstein m⁻² s⁻¹ by following the reference of Thimijan et al. (1983). Water in the water bath was renewed through a continuous flow to maintain the average in situ temperature (≈28°C). The bottles were mixed gently once per day. After 72 hours, thick phytoplankton growth was noticed dominated by diatoms like *Chaetoceros*, *Leptocylindrus*, *Nitzschia* and *Pseudo-nitzschia*. Please note that we do not claim to represent a natural community for this experiment, however this diatom composition is consistent with the most common bloom forming diatoms reported from this region.

Setting up the main experiment and carbon chemistry measurements:

A schematic plan of the experiment is shown in Fig. 2. Out of eight filled bottles with filtered seawater, four bottles were used as ambient CO₂ treatments (A-CO₂) without changing the carbon chemistry. During the filtration process, the CO₂ levels were equilibrated with the normal atmospheric CO₂ levels. High CO₂ treatments (H-CO₂) were achieved by bubbling pure CO₂ gas from a CO₂ cylinder in another four bottles with an acid cleaned tubing (Tygon). pH drop was initially monitored till 7.8 using a pre-calibrated pH meter (Systronics, India; with standard buffers of pH 4, 7 and 9 from Merck chemicals, USA). The targeted H-CO₂ levels were $\approx 1000\mu\text{atm}$. The final pH and pCO₂ values were calculated later using the total alkalinity (TA) and dissolved inorganic carbon (DIC) values. DIC and TA samples were collected immediately in acid cleaned glass bottles without head space and preserved with few drops of saturated HgCl₂ solution and stored at room temperature till analysis. TA was measured by potentiometric titration against 0.1N HCl using a pH meter (Systronics 362, India) (Bradshaw and Brewer, 1998). The Dickson international reference material (Batch 131) was used and the average error was < 2% of this measurement. DIC was measured using a coulometer attached to an acidification module (UIC-CM 5015) against the certified reference material (Dickson batch 170). The average error of this measurement was <5% during the analyses. CO₂SYS (Pierrot et al., 2006) was used (pH in NBS scale and K1, K2 from Mehrbach et al., 1973 refit by Dickson and Millero, 1987) to calculate the pCO₂ and pH values using TA and DIC value.

All bottles were filled without any headspace and kept closed for further trace metal and phytoplankton biomass addition. In Exp-I, Zn (1nM) was added from ZnSO₄ (Merck, Germany) stock solution prepared in trace metal free deionized water without any chelating agent. Thus, a total four sets of bottles in triplicate were made as follows: 1) A-CO₂, 2) A-CO₂+Zn, 3) H-CO₂ and 4) H-CO₂+Zn (Fig. 1c). Only one Zn level was used because the phytoplankton biomass was not enough to repeat another level with replicate. In Exp-II, three different concentrations (1nM, 2nM and 8nM) of Cu (from standard CuCl₂, 2H₂O solution) were used in both A-CO₂ and H-CO₂ mediums (Fig. 2). Finally, the phytoplankton biomass (10ml) was added to each bottle inside a clean bench with the help of a sterile pipette and kept closed. These bottles were incubated inside the water bath following the same protocol as followed for the stock culture. Each bottle was mixed gently everyday by 10:00 am to avoid biomass settling at the bottom. After 3 days of incubation, subsamples were collected from each bottle for all parameters and preserved for analysis. Nutrients were analyzed onboard following the standard colorimetric protocols (Grasshoff et al., 2009) using a Spectrophotometer (UV-Vis 1800, Shimadzu, Japan).

Chla was determined by fluorometric method (Strickland and Parsons, 1972) using a Turner's fluorometer (Trilogy R Laboratory Fluorometer) and Chla standard (Sigma Aldrich, USA). Phytoplankton cell density was counted using 3ml of preserved sample (Lugol's iodine; 1%; w/v) in an Utermohl counter (Hydrobias Kiel, Germany) under a Nikon (Ti2) inverted microscope. Growth rate was calculated using the following formula:

Growth rate ($\mu_{\text{cell based day}^{-1}}$) = [LN (Final cell number) – LN (Initial cell number)]/day.

Cellular carbohydrate content was determined spectrophotometrically following the method of Hedge et al. (1962) using sulfuric acid-Anthrone. Cellular protein content was estimated following Lowry's colorimetric method (Lowry et al., 1951) using Folin-Ciocalteu's solution. POC and $\delta^{13}\text{C}_{\text{POC}}$ were analyzed following the protocol of Sharp et al. (1974) using an elemental analyzer (Thermo Fisher, Flash HT) coupled to an isotopic ratio mass spectrometer (Thermo Fisher, Delta) against the standard reference materials from NIST, Maryland, USA at Alyses analytical platform (Bondy, France). The certified value for $\delta^{13}\text{C}$ was traceable to IAEA-CH-6 (IAEA, Vienna) (calibrated to Vienna PDB). The results of $\delta^{13}\text{C}_{\text{POM}}$ were calculated using the following formula:

$$\delta^{13}\text{C}_{\text{POC}} = [\{ (^{13}\text{C}/^{12}\text{C})_{\text{sample}} / (^{13}\text{C}/^{12}\text{C})_{\text{standard}} \} - 1] * 1000$$

Biogenic Silica (BSi) content was analyzed spectrophotometrically following the method described by Paasche (1973).

Two-factor ANOVA (with replication) tests were carried out to check the level of significance (95%) and probability values (p) against the impacts of increasing CO_2 supply as well as Cu and Zn on phytoplankton community.

Results

The initial and final values of carbon chemistry parameters along with nutrients concentrations are shown in Table 1. The initial dissolved Zn and Cu concentrations were $4.7 \pm 1.4 \text{ nM}$ and $11 \pm 3 \text{ nM}$, respectively. Both experiments started with a very low cell density as targeted ($< 100 \text{ cells mL}^{-1}$). After 3rd day of incubation, a thick algal biomass developed coupled with depleted nutrient concentrations in all media of both experiments. The targeted pCO_2 value was close to $1000 \mu\text{atm}$ (pH 7.8). In Exp-I, the estimated pCO_2 was $\approx 400 \mu\text{atm}$ in the A- CO_2 (pH of 8.17) and $943 \mu\text{atm}$ in H- CO_2 (pH 7.87) treatments (Table 1). During Exp II, the CO_2 level was $\approx 400 \mu\text{atm}$ (pH 8.17) under A- CO_2 and $\approx 1000 \mu\text{atm}$ (pH 7.84) in the H- CO_2 treatments (Table 1). Like other closed batch culture experiments, here also significantly increased pH values were noticed in the final samples. In Exp-I, the magnitude of pH enhancement was relatively higher than it was noticed in Exp-II (Table

1). The difference between the final pH/pCO₂ values of A-CO₂ and H-CO₂ treatments was quite small. This may lead to a question that if the observed growth response in the final samples can still be attributed to variable CO₂ levels. However, we argue that the maximum growth/biomass accumulation takes place during the log phase (usually noticed on day 3 for our coastal phytoplankton communities), followed by nutrient exhaustion and cessation of growth. We collected the samples on 4th day which is likely to be the end of log phase and beginning of the decelerating phase. Therefore this is likely that till the log phase, pH values remained stable and decreased only after major photosynthetic DIC drawdown happened. This means that the major part of biomass development occurred before pH value increased at H-CO₂ levels and the impacts of two different CO₂ level are still valid for this experiment.

The results are discussed individually in relation to CO₂ and trace metals in the following sections.

Exp I

Impacts of CO₂

In Exp-I, H-CO₂ treatment exhibited a higher ($p < 0.05$) cell density (Fig. 3a) and growth rate (Fig. 3b) than that of A-CO₂ level. The bulk Chl_a concentrations (Fig. 3c), Chl_a per cell content (Fig. 3d) and total carbohydrate (Fig. 3e) concentrations did not show any appreciable difference in response to varying CO₂ level. However, carbohydrate content per cell (Fig. 3f) decreased by 48% under H-CO₂ condition (23.2 ± 7.9 pg cell⁻¹) compared to A-CO₂ treatment (44.8 ± 6.3 pg cell⁻¹). But this trend was not statistically significant ($p > 0.05$). Protein concentrations (Fig. 3g) were not considerably different between A-CO₂ and H-CO₂ treatments but CO₂ seemed to increase protein contents per cell (Fig. 3h) and decrease carbohydrate to protein ratio (Fig. 3i) ($p < 0.01$). Total POC concentrations (Fig. 3j) and POC content per cell (Fig. 3k) in A-CO₂ treatment were 186 ± 17 μmol L⁻¹ and 57.13 ± 6.05 pg C cell⁻¹, respectively and these values showed slight reduction under H-CO₂ treatment (164 ± 9.4 μmol L⁻¹; 32.3 ± 3.2 pg C cell⁻¹) however, the two-factor ANOVA revealed no significant trend ($p > 0.05$). The concentrations of BSi (Fig. 3l) and BSi content per cell (Fig. 3m) were 6.3 ± 3.7 μmol L⁻¹ and 150 ± 63 fmol cell⁻¹, respectively under A-CO₂ level. These values did not show any statistically significant difference under H-CO₂ level. δ¹³C_{POM} ($-20.911 \pm 0.67\%$) values from A-CO₂ treatment (Fig. 3n) did not show any significant change under H-CO₂ treatment ($-20.45 \pm 0.35\%$).

Impact of Zn

Zn addition under A-CO₂ treatment did not exert any significant change in cell number (Fig. 3a), growth rate (Fig. 3b) and Chl*a* concentration (Fig. 3c). On the contrary, under H-CO₂ treatment, addition of Zn resulted in 2.5 times decreased cell density and 15% reduction in growth rate ($p < 0.05$). Chl*a* content per cell remained unchanged in response to Zn addition under A-CO₂ levels but the combined effects of increasing CO₂ and Zn addition resulted in an increase of 139% of Chl*a* content per cell (Fig. 3d) ($p < 0.05$). Zn addition showed no significant difference in total carbohydrate concentration (Fig. 3e) and carbohydrate content per cell (Fig. 3f) in any CO₂ level. Total protein concentrations (Fig. 3g) and protein contents per cell (Fig. 3h) were not affected by Zn addition under A-CO₂ level. However, they increased significantly from 14.6 ± 3 pg cell⁻¹ to 50.4 ± 8.4 pg cell⁻¹ after the addition of Zn under H-CO₂ treatment ($p < 0.001$). The carbohydrate to protein ratio (Fig. 3i) under A-CO₂ (2.04 ± 0.6) and A-CO₂+Zn (1.9 ± 0.5) were not significantly different ($p > 0.05$). Conversely, H-CO₂+Zn treatment showed 42% decrease in carbohydrate to protein ratio than that found in H-CO₂ level ($p < 0.05$). BSi concentrations (Fig. 3j) and BSi contents per cell (Fig. 3k) in A-CO₂ and H-CO₂ treatment were almost similar when Zn was added. Total POC concentrations (Fig. 3l) and POC contents per cell (Fig. 3m) did not vary in response to Zn addition under A-CO₂ level; however, under H-CO₂ level, Zn addition showed a significant increase in POC content cell⁻¹ (Fig. 3m). $\delta^{13}\text{C}_{\text{POM}}$ was $-20.91 \pm 0.67\text{‰}$ (Fig. 3n) under A-CO₂ treatment and did not change significantly after Zn addition ($-20.48 \pm 0.82\text{‰}$). Under H-CO₂ level this value was $-20.45 \pm 0.35\text{‰}$ and showed -1.1‰ depletion in H-CO₂+Zn treated samples, however, this change was not statistically significant ($p > 0.05$).

Exp II: Impacts of CO₂

In this experiment, cell density (Fig. 4a), growth rate (Fig. 4b), Chl*a* concentrations (Fig. 4c), per cell Chl*a* content (Fig. 4d), total carbohydrate concentrations (Fig. 4e) and per cell carbohydrate content (Fig. 4f) did not show any significant difference in response to increasing CO₂ levels ($p > 0.05$). Similarly, total protein concentrations (Fig. 4g) and protein contents per cell (Fig. 4h) showed insignificant change between A-CO₂ to H-CO₂ treatments. Carbohydrate to protein ratio (Fig. 4i) (0.91 ± 0.09) under H-CO₂ level was 31% ($p < 0.05$) lower than that of A-CO₂. BSi concentrations (Fig. 4j) along with BSi content per cell (Fig. 4k) did not show significant difference under A-CO₂ and H-CO₂ levels. POC concentrations in A-CO₂ (245 ± 39 μmol L⁻¹) and H-CO₂ treatment (236 ± 3 μmol L⁻¹) (Fig. 4l) and POC content per cell (Fig. 4m) did not differ significantly. The $\delta^{13}\text{C}_{\text{POM}}$ value was -23.59 ± 0.05 ‰ (Fig. 4n) under A-CO₂ treatment and increasing CO₂ supply showed a slight but not significant depletion under H-CO₂ level ($-23.66 \pm 0.3\text{‰}$). The average values

of $\delta^{13}\text{C}_{\text{POM}}$ under A-CO₂ and ACO₂+Cu treated samples were relatively enriched than that of HCO₂ and HCO₂+Cu treated samples. Two-factor ANOVA showed that the impact of CO₂ was significant ($p < 0.05$).

Impacts of Cu

Cu addition exerted a significant difference in only few parameters (Fig. 4a -4n). 8nM Cu addition under H-CO₂ treatment enhanced per cell Chl*a* content from 171 ± 40 fg cell⁻¹ to 339 ± 49 fg cell⁻¹ ($p < 0.001$). A similar trend was also seen under A-CO₂ level. The two-factor ANOVA test showed this increase as significant ($p < 0.001$). Carbohydrate concentrations (Fig. 4e), carbohydrate content per cell (Fig. 4f), protein concentrations (Fig. 4g) were comparable under A-CO₂ and H-CO₂ levels with Cu addition. Two-factor ANOVA showed that Cu addition made strong impact on protein contents per cell (Fig. 4h) and carbohydrate to protein ratio (Fig. 4i) ($p < 0.01$). BSi concentrations did not show any significant change by Cu treatment under A-CO₂ and H-CO₂ levels (Fig. 4j). The slight decrease in BSi content per cell from H-CO₂ (1.5 ± 0.5 fmol cell⁻¹) (Fig. 4k) to H-CO₂+8nM Cu treated samples (2.4 ± 1.01 fmol cell⁻¹) was not statistically significant ($p > 0.05$). The final POC concentration was $\approx 200 \mu\text{mol L}^{-1}$; there was no significant impact of Cu addition (1nM - 8nM) (Fig. 4l) under A-CO₂ and H-CO₂ levels. POC content per cell (Fig. 4m) showed significant changes in response to Cu addition under A-CO₂ and HCO₂ levels ($p < 0.05$). The average $\delta^{13}\text{C}_{\text{POM}}$ value in the H-CO₂+Cu added samples (-23.8‰) more depleted from the values noticed under H-CO₂ (-23.66‰) (Fig. 4n) (). Under 8nM Cu treated samples in H-CO₂ condition, a significant depletion was noticed in $\delta^{13}\text{C}_{\text{POM}}$ values (-24.05‰); two-factor ANOVA results showed that Cu did not make any significant impact on $\delta^{13}\text{C}_{\text{POM}}$ values ($p > 0.05$).

Phytoplankton Community response

The phytoplankton community was mostly dominated by diatoms as confirmed by both microscopy and HPLC (data not shown here). Due to dilution effects the presence of grazers like small ciliates was minimized and microscopic examination showed no signs of ciliates in the incubations. Overall, in Exp-I, centric diatoms dominated (86%) the initial community and they remained dominant (74%) in the post incubation samples with slight reduction. The ratio of centric to pennate diatom was 6.14 and reduced to 3 under A-CO₂ and A-CO₂+Zn treatments. Hence, Zn addition under A-CO₂ treatment showed little or no impact on this ratio. Interestingly, under H-CO₂ levels, centric to pennate ratio was higher (> 4.1) indicating preferences of H-CO₂ by some centric diatoms. Two-factor ANOVA showed that CO₂ has significant impact on this ratio ($p < 0.001$). Microscopic analysis revealed that during Exp I, the initial phytoplankton community (Fig. 5a) was

dominated by *Chaetoceros* (79.3%) followed by *Pseudo-nitzschia*(7.3%), *Nitzschia* (5.47%), *Leptocylindrus* (4.7%) and *Skeletonema*(2.16%). In the post-incubated samples, *Chaetoceros* remained as a major genus, although its relative abundance decreased slightly ($\approx 10\%$) in all treatments (Fig. 5a). Interestingly, the toxigenic pennate diatom *Pseudo-nitzschia* abundance doubled under H-CO₂ and H-CO₂+Zn treated samples and tripled in A-CO₂ and A-CO₂+Zn treatments from its initial abundance. *Nitzschia* abundance decreased to almost half in all final samples. *Leptocylindrus* abundance also decreased to almost 30% in all the treatments, except under H-CO₂+Zn treated samples where it doubled than its initial value. *Skeletonema* showed more than 70% increase under A-CO₂ and A-CO₂+Zn treatments and 2 and 3 fold increase in H-CO₂ and H-CO₂+Zn treated samples, respectively from its initial value.

Exp-II was conducted one week after Exp-I and the phytoplankton stock culture was maintained under the same condition onboard. A significant change in the community took place within this gap and the pennate diatoms became the dominating group. Initially, in Exp-II the ratio of centric to pennate diatoms was 0.55. This ratio decreased to 0.23 ± 0.12 , 0.18 ± 0.03 , 0.21 ± 0.04 and 0.33 ± 0.39 at A-CO₂, A-CO₂+1nM Cu, A-CO₂+2nM Cu, A-CO₂+8nM Cu, respectively in the final samples. In the initial community (Fig. 5b) *Nitzschia* dominated (62%) followed by *Leptocylindrus* (34.5%), *Pseudo-nitzschia* (2%) and *Chaetoceros* (0.3%). *Nitzschia* showed 24% (Fig. 5b) higher abundance under A-CO₂ level and remained same as the initial value in all Cu-treated samples (Fig. 5b). The changes in centric to pennate ratios under H-CO₂ levels (0.35 ± 0.2 ; $0. \pm 0.19$; 0.31 ± 0.2 and 0.13 ± 0.06 at H-CO₂, H-CO₂+1nM Cu, H-CO₂+2nM Cu, H-CO₂+8nM Cu, respectively) were not significantly different ($p > 0.05$) from the values noted at A-CO₂ levels (with and without Cu). Contrary to Exp-I, neither Cu nor CO₂ levels showed statistically significant change in centric to pennate ratio. Under H-CO₂ levels, there were marginal changes in *Nitzschia* abundance without any significant trend. In this experiment the second abundant diatom was *Leptocylindrus* which decreased to half at the end of experiment in both A-CO₂ and A-CO₂+Cu treated samples. In the H-CO₂ treatment, *Leptocylindrus* showed almost 32% decrease followed by a sharp decline (23 to 9%) under H-CO₂+Cu treated samples. *Pseudo-nitzschia* was one of the least abundant species in this experiment and showed comparable abundance under initial and A-CO₂ level. This genus showed 8-10 times increased abundance in all Cu-treated samples under both CO₂ levels. In H-CO₂, H-CO₂+1nM Cu, H-CO₂+2nM Cu and H-CO₂+8nM Cu-treated samples, there were 4, 14, 9 and 7 times increase in *Pseudo-nitzschia* abundance, respectively from its initial value. *Chaetoceros* was the least abundant species and became almost undetectable under A-CO₂ treatment and at very low concentration in all Cu treated samples ($< 1\%$). Under H-CO₂ level, *Chaetoceros* abundance

decreased by 33% and increased again by 2.5 to 8 times in the H-CO₂+ Cu treated samples. These changes resulted in an increase of the centric to pennate diatom ratio to 0.2 and 0.35 under A-CO₂ and H-CO₂ treatments. Addition of Cu under A-CO₂ level did not show any significant trend in this ratio. The addition of 1 and 2nM Cu under H-CO₂ level showed negligible changes of centric to pennate ratio which was reduced to 0.13 under H-CO₂+8nMCu treatment with highest (83.8%) pennate diatom abundance.

Discussion

Phytoplankton community response to increasing CO₂

Phytoplankton community compositions were quite different during the two experiments. In both the experiments the effect of elevated CO₂ level/lower pH neither showed any significant beneficial impact nor any growth inhibition on the phytoplankton community. However there were significant changes in the community composition clearly indicating that increasing CO₂ levels can favor certain phytoplankton species. Similarly, the addition of Zn and Cu may facilitate different diatom species under low pH condition. Phytoplankton from coastal, upwelling and estuarine waters are expected to be well acclimatized to a wide range of pH and CO₂ levels (Bénard et al., 2018; Li, Wu, Hutchins, Fu and Gao, 2016). In Exp-I, CO₂ induced increase of cell density was probably due to enhanced rate of cell division of the dominating centric diatoms *Chaetoceros*, *Leptocylindrus* and *Skeletonema* whilst, in Exp-II *Leptocylindrus* showed higher abundance at elevated CO₂ level. Such CO₂ dependent community shift indicated that under elevated CO₂ level, the centric diatoms probably gained some energetic benefit to outcompete the smaller species. Replacement of small pennate diatom (*Cylindrotheca*) by the large centric diatom (*Chaetoceros*) under elevated CO₂ level was also reported by Feng et al., (2010) and Tortell et al. (2008) noticed a similar trend where the small pennate diatom (*Pseudo-nitzschia*) was replaced by *Chaetoceros* under H-CO₂ condition. Under a low pCO₂ level in surface water smaller pennates may grow better with higher surface area to volume ratios which possibly help to ease DIC acquisition (Tortell et al., 2008). This also explains the higher centric:pennate ratio, observed under elevated CO₂ levels. During Exp-II, the absence of increased cell division was probably due to a different diatom community dominated by pennates.

Impact of increasing CO₂ on phytoplankton growth

In the present experiment, there was no signature of enhanced photosynthesis or growth stimulation on any of the biomass indicators (POC, protein, carbohydrate, Chl_a) due to CO₂ enrichment. Insignificant changes in BSi contents along with POC to BSi ratios under H-CO₂ levels indicated negligible impact of changing CO₂ levels on the growth and physiology of this

phytoplankton community. A similar response was also noticed in other studies (Feng et al., 2009; Li and Campbell, 2013; Li et al., 2016; Shaik et al., 2017; Biswas et al., 2017). The impacts of increasing CO₂ supply on phytoplankton photosynthetic performances are directly linked to DIC acquisition and its energy costs. The main carboxylating enzyme RubisCO shows very low affinity towards CO₂ (Falkowski and Raven, 2007) and the half saturation constant of RubisCO for CO₂ is almost 40 μmol kg⁻¹ (Badger et al., 1998). However, the concentrations of dissolved CO₂ in the surface oceans are only 10-12 μmol kg⁻¹ and thus may limit optimum photosynthesis in marine phytoplankton (Riebesell et al., 1993). Nevertheless, this may largely depend on the diatom species dominating the community since there is a high diversity in diatom Carbon Concentration Mechanisms (CCMs; Young et al. 2016). Additionally, due to high concentration gradient across the cell wall, a significant amount of cellular CO₂ can be lost through diffusion. In order to attain optimal photosynthetic rate, marine phytoplankton developed CCMs, an energy consuming process to increase CO₂ level in the vicinity of RubisCO (Badger et al., 1998; Reinfelder, 2011). In this process phytoplankton cells accumulate DIC in the form of bicarbonate ions (HCO₃⁻) at the cost of energy (Reinfelder, 2011). Therefore, it has been hypothesized that ongoing increase in the CO₂ levels may enhance diffusive CO₂ influx as well as reduce CO₂ loss from the cell and the CCMs related energetic costs can be down regulated (Sommer et al., 2015) leading to higher growth (Reinfelder, 2011). However, the experimental evidences from different marine habitats reported highly diverse responses of phytoplankton to increasing CO₂ levels.

A number of laboratory-based studies showed an enhanced photosynthetic rate, storage carbohydrate and POC contents (Biddanda and Benner, 1997; Biswas et al., 2017; Shaik et al., 2017) in response to increasing CO₂ level in marine phytoplankton. But at the same time, many authors reported that under elevated CO₂ condition, the growth and photosynthetic rate of marine phytoplankton remained unaltered (Eberlein et al., 2017; Feng et al., 2009; Gao et al., 2017; Hoppe; Keys et al., 2018; Zhang et al., 2018). Recently, Hoppe et al., (2018) have shown that the Arctic phytoplankton species displayed extreme plasticity to changing CO₂ levels and seem to have a strong cellular mechanism to counteract the impacts of OA. Likewise, the present experimental community showed high resilience to increasing CO₂ levels with equal amount of carbon biomass accumulated under A-CO₂ and H-CO₂ levels. Further, no significant depletion of δ¹³C_{POM} values in response to the increased CO₂ levels in the first experiment suggest that DIC was possibly consumed as bicarbonate ions but not as dissolved CO₂. Less discrimination in δ¹³C_{POM} values is usually seen when grown on bicarbonate e.g. as in coastal diatoms (Tortell et al., 2002). This observation also suggested that upon the supply of increasing CO₂, the cells probably did not make any energetic savings and hence, there

was no energetic benefit related to CCM cost down regulation. Conversely, during the second experiment, H-CO₂ seemed to induce depleted $\delta^{13}\text{C}_{\text{POM}}$ values; however, this may be also due to slower growth while countering the low pH effect and change in the community composition. Since dark respiration rate was not measured, this is difficult to state how the community responded to low pH. Nevertheless, it is clear that phytoplankton cells were well acclimatized to a CO₂ enriched environment probably as a result of living in an upwelling area for a prolonged time. Hence, the projected CO₂ levels may not alter the photosynthetic performance in this phytoplankton community.

Impacts of Zn addition

The addition of Zn under A-CO₂ condition showed insignificant effects on growth and community structure of the experimental phytoplankton community. This suggested that Zn has neither growth stimulating nor inhibitory effects. Excess of Zn did not alter the centric to pennate ratio either in A-CO₂ or H-CO₂ levels. However, additional Zn supply was found to be deleterious for cell division in H-CO₂ treatment. The binding of trace metal ions to the cell surface and their uptake is controlled by H⁺ concentrations (Macfie et al., 1994). Increase in Zn bioavailability with decreasing pH was reported in coastal waters by Kim et al. (2016). Under low pH, the bioavailability of Zn may increase due to the competition of natural ligands and H⁺ ions to bind with the metal ion (Millero et al., 2009). When the concentrations of H⁺ increase, there will be simultaneous release of free Zn ions that may potentially increase cell bound Zn ions and can inhibit cell division. Usually, cell membrane bound Zn ions interrupt Ca uptake and thus inhibit the Ca-ATPase activity necessary for cell division (Stauber and Florence, 1990). In contrast, the photosynthetic rate was unaffected with excess Zn. The drawdown of DIC under low pH/high CO₂ levels with and without Zn addition was comparable supporting that Zn addition did not inhibit carbon uptake and photosynthetic rates. However, the fixed carbon was accumulated within the cells since they could not divide and resulted in the accumulation of photosynthetic products and increase of cell size. This also explains for significantly higher Chl_a, protein and POC contents per cell under H-CO₂+Zn treatments. The metal treated cells presumably enlarged because of an uncoupling between photosynthetic and cell division rates (Fisher et al., 1981). Addition of Zn was shown to reduce the cell division rate by half at 1nM level in the marine diatom, *Nitzschia closterium*; however, the photosynthetic and respiratory performances still remained unaffected even when the concentration raised up to 7nM (Stauber and Florence, 1990). Slow growth rate was also supported by the depleted values of $\delta^{13}\text{C}_{\text{POM}}$ (Burkhardt et al., 1999) under H-CO₂+Zn than that of only H-CO₂ treatment. Considerable increase in protein concentration under H-CO₂+Zn treatment suggested synthesis of some stress related protein in order to reduce metal toxicity. Rijstenbil et al. (1994) reported that Zn may indirectly stimulate antioxidant

protein activity in marine diatom. Stauber and Florence, (1990) also reported an enhanced production of thiol (SH) and glutathione concentrations in the Zn treated cells as compared to the untreated cells. Moreover, the energy required to detoxify cellular Zn may also toll on the energy that is allocated to cell division (Stauber and Florence, 1990).

Here, increased abundance of the centric diatoms *Leptocylindrus* and *Skeletonema* under H-CO₂+Zn treatment indicated that these diatoms can counteract Zn toxicity and may also benefit from Zn addition. *Pseudo-nitzschia* showed higher sensitivity to Zn toxicity under H-CO₂ level; whereas, *Chaetoceros* revealed higher tolerance to Zn relative to other species. Dominance of *Skeletonema* under H-CO₂+Zn treatment was also found in the samples from Bay of Bengal (Biswas et al., 2017). *Skeletonema* and *Chaetoceros* bloom was reported from polluted harbors (Raman, 1995) and coastal waters (Shaik et al., 2015) indicating their ability to tolerate high pollutant level.

Impacts of Cu addition

Cu stress can be highly deleterious for algal cells in general (Morin et al. 2012; Masmoudi et al. 2013; Lopez et al. 2019) and physiological functioning can be hindered to a considerable level in marine diatoms (Manimaran et al. 2012; Morin et al. 2012). However, in the present experiment, unlike Zn, the treatment with excess Cu at A-CO₂ and H-CO₂ levels seemed to exert no significant impact on phytoplankton growth. In both CO₂ levels, the concentrations of Chl_a, POC and carbohydrate were comparable among different Cu treated samples suggesting no significant impact of Cu on photosynthetic performance. Dissolved Cu concentration in the experimental seawater was quite high (11 nM). Rejomon et al (2009) reported almost double values of Cu and Zn concentrations in the shelf waters of AS (close to our sampling stations) during Sept-Oct. The phytoplankton community seemed to be well acclimatized to such Cu concentrations and probably therefore no major changes in the growth rate and photosynthetic performance was noticed. Usually, at elevated Cu levels, the generation of reactive oxygen species (ROS) inside algal cell may create high oxidative stress (Knauert and Knauer, 2008; Masmoudi et al. 2013). As a defense mechanism, diatoms synthesize various antioxidant proteins (Manimaran et al. 2012) which were also noticed in a coastal diatom under Cu stress from SW coast of India (Anu et al., 2016). In the present experiment, the increased per cell protein contents and reduced carbohydrate to protein ratio in H-CO₂+Cu treated cells could be due to synthesizing such proteins.

At toxic levels, Cu can significantly inhibit silicate uptake rate in marine diatoms (Manimaran et al. 2012) because Cu and Si compete for the same protein transporter during the cellular transport process (Morel et al., 1978; Rueter et al., 1981). Particularly, when Si:Cu ratio

decreases due to increasing Cu levels, the chances of inhibition is more. Earlier studies also showed that at elevated Cu levels, BSi formation was significantly hampered (Biswas et al., 2013; Biswas and Bandyopadhyay, 2017). However, in this study imperceptible reduction in BSi concentrations and cellular BSi quota in response to Cu addition under A-CO₂ and H-CO₂ levels also suggested insignificant toxic impacts of Cu on silicate uptake and its metabolism in the experimental phytoplankton community. The POC to BSi ratio remained unchanged suggesting photosynthetic carbon accumulation and silicification were mostly unaffected by the experimental conditions. Thus, this finding supported the view that the experimental diatoms community possesses the physiological mechanisms to counteract Cu toxicity probably due to living in a Cu enriched environment

Albeit of the fact that Cu did not impact phytoplankton growth in general, the impacts on community shift was considerable. The physiological responses of diatoms to metal contaminations are usually alike, however, the responses of the community seem to be different (Morin et al. 2012). The combined effects of Cu pollution and OA have been shown to be detrimental for the early microscopic life stage of a kelp species (Leal et al., 2018). The centric diatom *Leptocylindrus* showed high sensitivity to both H-CO₂ and Cu. In contrast, the pennate diatom *Nitzschia* showed its high potential to cope-up with elevated Cu levels and could be the reason for forming bloom in the upwelling and polluted waters (Morin et al. 2012). In our study, the abundance of toxigenic pennate diatom *Pseudo-nitzschia* showed significant increase with increasing Cu levels under both A-CO₂ and H-CO₂ treatments showing its higher level of acclimatization capability under Cu stress. The potential algal toxin, domoic acid, produced by *Pseudo-nitzschia*, is a Cu chelator (Lelong et al., 2012) and this probably helps them to survive under high Cu concentrations (Lelong et al., 2012). Schnetzer et al., (2013) reported the occurrences of consecutive *Pseudo-nitzschia* bloom in relation to upwelling events in the Los Angeles coastal waters. Both H-CO₂ and elevated Cu levels have shown to facilitate *Pseudo-nitzschia* growth (Feng et al., 2009; Lelong et al., 2012; Tatters, Fu and Hutchins, 2012). Sun et al. (2011) showed that domoic acid producing strain of *Pseudo-nitzschia* responded positively to increasing CO₂ levels. Moring et al. (2017) monitored the combined effects of Cu toxicity and warming on a diatom biofilm over a six weeks period. The authors observed that the toxic impacts of Cu were intensified under future warming scenario showing the possibility of increasing metal toxicity in a future warmer world. These observations collectively indicate that increasing Cu pollution along with OA and other stresses like warming or nutrient limitation may introduce significant changes in the diatom diversity. The growth of the toxin producing species like *Pseudo-nitzschia* can be facilitated in future in coastal waters and may adversely impact the ecosystem (Feng et al., 2009; Wells et al. 2015). More experimental evidences are necessary to

precisely assess the impacts of the projected increase in coastal pollution combined with the projected changes of temperature, carbon chemistry and pH.

Acknowledgements

We are thankful to the Director, CSIR-NIO for his active support. We thank the Council of Scientific and Industrial Research (CSIR) and Department of Science and Technology (DST) for providing funds. The French Institute for Research and Development (IRD) is acknowledged for the funding of POC and isotopic analyses. We also thankfully acknowledge the generous contribution of two anonymous reviewers. The active technical support from the captain, crew members, and ship-cell members of SSD-40 are also gratefully acknowledged. CSIR-NIO contribution No. is XXXX.

References:

1. Anu, P. R., Bijoy Nandan, S., Jayachandran, P. R. and Xavier, N. D. D., 2016, Toxicity effects of copper on the marine diatom, *Chaetoceros calcitrans*, Regional Studies in Marine Science 8, 498-504.
2. Bach, L.T., Alvarez-Fernandez, S., Hornick T., Stuhr A. Riebesell, U., 2017. Simulated ocean acidification reveals winners and losers in coastal phytoplankton. PloSOne 12(11), 188-198.
3. Badger, M. R., Andrews, T. J., Whitney, S. M., Ludwig, M., Yellowlees, D. C., Leggat, W., Price, G. D., 1998) The diversity and coevolution of Rubisco, plastids, pyrenoids, and chloroplast-based CO₂-concentrating mechanisms in algae. Canadian Journal of Botany 76(6), 1052-1071.
4. Bénard, R., Lévassieur, M., Scarratt, M., Blais, M.A., Mucci, A., Ferreyra, G., Starr, M., Gosselin, M., Tremblay, J.É., Lizotte, M., 2018. Experimental assessment of the sensitivity of an estuarine phytoplankton fall bloom to acidification and warming. Biogeosciences 15(16), 4883-4904.
5. Biddanda, B. and Benner, R., 1997. Carbon, nitrogen, and carbohydrate fluxes during the production of particulate and dissolved organic matter by marine phytoplankton. Limnology and Oceanography 42(3), 506-518.
6. Biswas, H. and Bandyopadhyay, D., 2017. Physiological responses of coastal phytoplankton (Visakhapatnam, SW Bay of Bengal, India) to experimental copper addition. Marine Environmental Research 131, 19-31.
7. Biswas, H., Bandyopadhyay, D., Waite A., 2013. Copper addition helps alleviate iron stress in a coastal diatom: response of *Chaetoceros gracilis* from the Bay of Bengal to experimental Cu and Fe addition. Marine Chemistry 157, 224-232.
8. Biswas, H., Shaik, A. U. R., Bandyopadhyay, D., Chowdhury, N., 2017. CO₂ induced growth response in a diatom dominated phytoplankton community from SW Bay of Bengal coastal water. Estuarine, Coastal and Shelf Science 198, 29-42.
9. Boyd, P.W., Collins, S., Dupont, S., Fabricius, K., Gattuso, J.P., Havenhand, J., Hutchins, D.A., Riebesell, U., Rintoul, M.S., Vichi, M. and Biswas, H. et al., 2018. Experimental strategies to assess the biological ramifications of multiple drivers of global ocean change—A review. Global Change Biology 24(6), 2239-2261.
10. Boyd, P.W., Hutchins, D.A., 2012. Understanding the responses of ocean biota to a complex matrix of cumulative anthropogenic change. Marine Ecology Progress Series 470, 125-135.
11. Bracken, M.E., Silbiger, N.J., Bernatchez, G. and Sorte, C.J., 2018. Primary producers may ameliorate impacts of daytime CO₂ addition in a coastal marine ecosystem. Peer J 6, 4739.

12. Bradshaw, A. L., Brewer, P. G., 1988. High precision measurements of alkalinity and total carbon dioxide in seawater by potentiometric titration. 2. Measurements on standard solutions. *Marine Chemistry* 24(2), 155-162.
13. Brown, N.E., Milazzo, M., Rastrick, S.P., Hall-Spencer, J.M., Therriault, T.W., Harley, C.D. 2018. Natural acidification changes the timing and rate of succession, alters community structure, and increases homogeneity in marine biofouling communities. *Global Change Biology* 24(1), 112-127.
14. Burkhardt, S., Riebesell, U., Zondervan, I., 1999. Effects of growth rate, CO₂ concentration, and cell size on the stable carbon isotope fractionation in marine phytoplankton. *Geochimica et Cosmochimica Acta* 63(22), 3729-3741.
15. Chan, F., Barth, J.A., Blanchette, C.A., Byrne, R.H., Chavez, F., Cheriton, O., Feely, R.A., Friederich, G., Gaylord, B., Gouhier, T., Hacker, S., 2017. Persistent spatial structuring of coastal ocean acidification in the California Current System. *Scientific Reports* 7 (1), 2526.
16. DeVries, T. (2014). The oceanic anthropogenic CO₂ sink: Storage, air-sea fluxes, and transports over the industrial era. *Global Biogeochemical Cycles*, 28(7), 631-647.
17. DeVries T., Holzer M., Primeau F. 2017. Recent increase in oceanic carbon uptake driven by weaker upper-ocean overturning. *Nature* 542(7640), 215.
18. Eberlein, T., Wohlrab, S., Rost, B., John, U., Bach, L. T., Riebesell, U., & Van de Waal, D. B. (2017). Effects of ocean acidification on primary production in a coastal North Sea phytoplankton community. *PLoS One*, 12(3), e0172594.
19. Falkowski, P. G., Raven, J. A., 2007. Photosynthesis and primary production in nature. *Aquatic photosynthesis* 2nd ed. Princeton University Press, Princeton.
20. Feely, R.A., Sabine, C.L., Lee K., Berelson, W., Kleypas, J., Fabry, V.J., Millero, F.J. 2004. Impact of anthropogenic CO₂ on the CaCO₃ system in the oceans. *Science* 305 (5682), 362-366.
21. Feng, Y., Hare, C. E., Leblanc, K., Rose, J. M., Zhang, Y., DiTullio, G. R., Nemcek, N. 2009. Effects of increased pCO₂ and temperature on the North Atlantic spring bloom. I. The phytoplankton community and biogeochemical response. *Marine Ecology Progress Series* 388, 13-25.
22. Feng, Y., Hare, C. E., Rose, J. M., Handy, S. M., DiTullio, G. R., Lee, P. A., Zhang, Y., 2010. Interactive effects of iron, irradiance and CO₂ on Ross Sea phytoplankton. *Deep Sea Research Part I: Oceanographic Research Papers* 57(3), 368-383.
23. Fisher, N. S., Jones, G. J., Nelson, D. M., 1981. Effects of copper and zinc on growth, morphology, and metabolism of *Asterionella japonica* (Cleve) 1. *Journal of Experimental Marine Biology and Ecology* 51(1), 37-56.
24. Gao, G., Jin, P., Liu, N., Li, F., Tong, S., Hutchins, D. A., Gao, K. 2017. The acclimation process of phytoplankton biomass, carbon fixation and respiration to the combined effects of elevated temperature and pCO₂ in the northern South China Sea. *Marine Pollution Bulletin* 118(1-2), 213-220.
25. Gaonkar, C. V., Ashwini, K., Matta, V. M. and Kurian, S., 2019. Assessment of crustal element and trace metal concentrations in atmospheric particulate matter over a coastal city in the Eastern Arabian Sea. *Journal of the Air & Waste Management Association*, DOI: 10.1080/10962247.2019.1680458.
26. Grasshoff, K., Kremling, K., Ehrhardt, M. (Eds.). 2009. *Methods of seawater analysis*. John Wiley and Sons, Inc.
27. Haigh, R., Ianson, D., Holt, C.A., Neate, H.E., Edwards, A.M., 2015. Effects of ocean acidification on temperate coastal marine ecosystems and fisheries in the Northeast Pacific. *PLoS One* 10(2), 117533.
28. Hedge, J. E., Hofreiter, B. T., Whistler, R. L. 1962. *Carbohydrate chemistry*. Academic Press, New York, 17.

29. Hester, K.C., Peltzer, E.T., Kirkwood, W.J., Brewer, P.G., 2008. Unanticipated consequences of ocean acidification: A noisier ocean at lower pH. *Geophysical Research Letters* 35(19).
30. Hoppe, C.J.M., Wolf, K.K., Schuback, N., Tortell, P.D., Rost, B., 2018. Compensation of ocean acidification effects in Arctic phytoplankton assemblages. *Nature Climate Change* 8, 529.
31. Hurd, C.L., Lenton, A., Tilbrook, B., Boyd, P.W., 2018. Current understanding and challenges for oceans in a higher-CO₂ world. *Nature Climate Change* 8, 686-694.
32. IPCC, 2013: Climate Change 2013: The Physical Science Basis. Contribution of Working Group I to the Fifth Assessment Report of the Intergovernmental Panel on Climate Change [Stocker, T.F., D. Qin, G.-K. Plattner, M. Tignor, S.K. Allen, J. Boschung, A. Nauels, Y. Xia, V. Bex, P.M. Midgley (Eds.)]. Cambridge University Press, Cambridge, United Kingdom and New York, NY, USA, 1535.
33. Kalapureddy, M.C.R., Kaskaoutis, D.G., Ernest, Raj, P., Devara, P.C.S., Kambezidis, H.D., Kosmopoulos, P.G., Nastos, P.T. 2009. Identification of aerosol type over the Arabian Sea in the pre-monsoon season during the Integrated Campaign for Aerosols, Gases and Radiation Budget (ICARB). *Journal of Geophysical Research: Atmospheres* 114(D17).
34. Keys, M., Tilstone, G., Findlay, H. S., Widdicombe, C. E., Lawson, T. 2018. Effects of elevated CO₂ and temperature on phytoplankton community biomass, species composition and photosynthesis during an experimentally induced autumn bloom in the western English Channel. *Biogeosciences* 15(10), 3203-3222.
35. Knauert, S. and Knauer, K., 2008. The role of reactive oxygen species in copper toxicity to two freshwater green algae. *Journal of Phycology* 44, 311 -319.
36. Kroeker, K.J., Gambi, M.C., Micheli, F., 2013a. Community dynamics and ecosystem simplification in a high-CO₂ ocean. *Proceedings of the National Academy of Sciences* 110(31), 12721-12726.
37. Kroeker, K.J., Kordas, R.L., Crim, R., Hendriks, I.E., Ramajo, L., Singh, G.S., Duarte, C.M., Gattuso, J.P. 2013b. Impacts of ocean acidification on marine organisms: quantifying sensitivities and interaction with warming. *Global Change Biology* 19(6), 1884-1896.
38. Leal, P.P., Hurd, C.L., Sander, S.G., Armstrong, E., Fernández, P.A., Suhrhoff, T.J., Roleda, M.Y., 2018. Copper pollution exacerbates the effects of ocean acidification and warming on kelp microscopic early life stages. *Scientific Reports* 8(1), 14763.
39. Lelong, A., Hégaret, H., Soudant, P., and Bates, S. S., 2012. *Pseudo-nitzschia* (Bacillariophyceae) species, domoic acid and amnesic shellfish poisoning: revisiting previous paradigms. *Phycologia* 51(2), 168-216.
40. Li F., Wu Y., Hutchins D. A., Fu F., Gao, K., 2016. Physiological responses of coastal and oceanic diatoms to diurnal fluctuations in seawater carbonate chemistry under two CO₂ concentrations. *Biogeosciences* 13(22), 6247-6259.
41. Li, G., Campbell, D. A., 2013. Rising CO₂ interacts with growth light and growth rate to alter photosystem II photoinactivation of the coastal diatom *Thalassiosira pseudonana*. *PLoS One* 8(1), 55562.
42. Lopez, J.S., Lee, L. and Mackey, K.R.M., 2019. The Toxicity of Copper to *Crocospaera watsonii* and Other Marine Phytoplankton: A Systematic Review. *Frontiers in Marine Science* 5, 511.
43. Lowry, O. H., Rosebrough, N. J., Farr, A. L., Randall, R. J., 1951. Protein measurement with the Folin phenol reagent. *Journal of Biological Chemistry* 193, 265-275.
44. Macfie, S.M., Tarmohamed, Y., Welbourn, P.M., 1994. Effects of cadmium, cobalt, copper, and nickel on growth of the green alga *Chlamydomonas reinhardtii*: the influences of the cell wall and pH. *Archives of Environmental Contamination and Toxicology* 27(4), 454-458.

45. Manimaran, K., Karthikeyan, P. Ashokekumar, S., Ashok Prabhu, V. and Sampathkumar, P., 2012. Effect of copper on growth and enzyme activities of marine diatom, *Odontella mobiliensis*. Bulletin of Environmental Contamination and Toxicology 88, 30-7.
46. Masmoudi, S., Nguyen-Deroche, N., Caruso, A., Ayadi, H., Morant-Manceau, A., Tremblin, G., 2013. Cadmium, Copper, Sodium and Zinc Effects on Diatoms: from Heaven to Hell — a Review," Cryptogamie Algologie 34(2), 185-225.
47. Millero, F. J., Woosley, R., Ditrolio, B., Waters, J., 2009. Effect of ocean acidification on the speciation of metals in seawater. Oceanography 22(4), 72-85.
48. Morel, N. M. L., Rueter, J. C., Morel, F. M. M., 1978. Copper toxicity to *Skletonema costatum* (Bacilaripphyceae). Journal of Phycology 14(1), 43-48.
49. Morin et al. 2012. Consistency in Diatom Response to Metal-Contaminated Environments. The Handbook and Environmental Chemistry, 19, Springer, Berlin, Heidelberg.
50. Morin, S., Lambert, A. S., Rodriguez, E. P., Dabrin, A., Coquery, M. Pesce, S. 2017. Changes in copper toxicity towards diatom communities with experimental warming. Journal of Hazardous Materials 334, 223-232.
51. Nriagu, J. O. 1989. A global assessment of natural sources of atmospheric trace metals. Nature 338:47.
52. Paasche, E. 1973. Silicon and the ecology of marine plankton diatoms. I. *Thalassiosira pseudonana* (*Cyclotella nana*) grown in a chemostat with silicate as limiting nutrient. Marine Biology 19(2), 117-126.
53. Pardew, J., Blanco, Pimentel, M., Low-Decarie, E., 2018. Predictable ecological response to rising CO₂ of a community of marine phytoplankton. Ecology and Evolution 8(8), 4292-4302.
54. Paytan, A., Mackey, K.R., Chen, Y., Lima, I.D., Doney, S.C., Mahowald, N., Labiosa, R., Post, A.F., 2009. Toxicity of atmospheric aerosols on marine phytoplankton. Proceedings of the National Academy of Sciences 106(12), 4601-4605.
55. Pierrot, D., Lewis, E., Wallace, D. W. R., 2006. MS Excel program developed for CO₂ system calculations. ORNL/CDIAC-105a. Carbon Dioxide Information Analysis Center, Oak Ridge National Laboratory, US Department of Energy, Oak Ridge, Tennessee.
56. Raman, A.V., 1995. Pollution effects in Visakhapatnam harbour, India: An overview of 23 years of investigations and monitoring. Helgoländer Meeresuntersuchungen 49(1), 633.
57. Reinfelder, J.R., 2011. Carbon concentrating mechanisms in eukaryotic marine phytoplankton. Annual Review of Marine Science 3(1), 291–325.
58. Rejomon, G., Balachandran, K. K, Nair, M., Joseoh, T., DineshKumar, C., Achuthankutty, T., Nair, K. K. C., and Pillai, N. G. K., 2009. Trace metal concentrations in Zooplankton from the Eastern Arabian Sea and Western Bay of Bengal. Environmental Frontiers 9(1): 22-32.
59. Reuter, Jr J. G., Chisholm, S. W., Morel, F. M. M. 1981. Effects of copper toxicity on silicic acid uptake and growth in *Thalassiosira pseudonana* [Algae]. Journal of Phycology. 17(3), 270-278.
60. Riebesell, U., 2004. Effects of CO₂ enrichment on marine phytoplankton. Journal of Oceanography 60(4), 719-729.
61. Riebesell, U., Wolf-Gladrow, D. A., Smetacek, V. 1993. Carbon dioxide limitation of marine phytoplankton growth rates. Nature 361(6409), 249.
62. Rijstenbil, J. W., Derksen, J. W. M., Gerringa, L. J. A., Poortvliet, T. C. W., Sandee, A., Van den Berg, M., Wijnholds, J. A., 1994. Oxidative stress induced by copper: defense and damage in the marine planktonic diatom *Ditylum brightwellii*, grown in continuous cultures with high and low zinc levels. Marine Biology 119(4), 583-590.

63. Rodushkin, I., Ruth, T., 1997. Determination of trace metals in estuarine and sea-water reference materials by high resolution inductively coupled plasma mass spectrometry. *Journal of Analytical Atomic Spectrometry* 12(10), 1181-1185.
64. Schnetzer, A. Jones, B.H., Schaffner, R.A., Cetinic, I., Fitzpatrick, E., Miller, P.E., Seubert, E.L., Caron, D.A., 2013. Coastal upwelling linked to toxic *Pseudo-nitzschia australis* blooms in Los Angeles coastal waters, 2005–2007. *Journal of Plankton Research* 35(5), 1080-1092.
65. Shaik, A.U.R., Biswas, H., Pal, S., 2017. Increased CO₂ availability promotes growth of a tropical coastal diatom assemblage (Goa coast, Arabian Sea, India). *Diatom Research* 32(3), 325-339.
66. Shaik, A.U.R., Biswas, H., Reddy, N. P. C., Rao, V. S., Bharathi, M. D., Subbaiah, C. V., 2015. Time series monitoring of water quality and microalgal diversity in a tropical bay under intense anthropogenic interference (SW coast of the Bay of Bengal, India). *Environmental Impact Assessment Review* 55, 169-181.
67. Sharp, J. H. 1974. Improved analysis for “particulate” organic carbon and nitrogen from seawater 1. *Limnology and Oceanography* 19(6), 984-989.
68. Shi, D., Xu, Y., Hopkinson, B.M., Morel, F.M., 2010. Effect of ocean acidification on iron availability to marine phytoplankton. *Science* 1183517.
69. Sommer, U., Paul, C., Moustaka-Gouni, M., 2015. Warming and ocean acidification effects on phytoplankton—from species shifts to size shifts within species in a mesocosm experiment. *PLoS One*, 10(5) 0125239.
70. Spilling, K., Paul, A. J., Virkkala, N., Hastings, T., Lischka, S., Stuhr, A., Bermúdez, R., Czerny, J., Boxhammer, T., Schulz, K. G., Ludwig, A., and Riebesell, U.: Ocean acidification decreases plankton respiration: evidence from a mesocosm experiment, *Biogeosciences*, 13, 4707–4719.
71. Stauber, J. L., Florence, T. M., 1990. Mechanism of toxicity of zinc to the marine diatom *Nitzschia closterium*. *Marine Biology* 105(3), 519-524.
72. Stockdale, A., Tipping, E., Lofts, S., Mortimer, R. J. G., 2016. Effects of ocean acidification on organic and inorganic speciation of trace metals. *Environmental Science and Technology* 50, 1906-1913.
73. Strickland, J. D., Parsons, T. R., 1972. A practical handbook of seawater analysis.
74. Sun, J., Hutchins, D. A., Feng, Y., Seubert, E. L., Caron, D. A., and Fu, F. X., 2011. Effects of changing pCO₂ and phosphate availability on domoic acid production and physiology of the marine harmful bloom diatom *Pseudo-nitzschia multiseriis*. *Limnology and Oceanography* 56(3), 829-840.
75. Tatters, A. O., Fu, F. X., Hutchins, D. A., 2012. High CO₂ and silicate limitation synergistically increase the toxicity of *Pseudo-nitzschia fraudulenta*. *PLoS One* 7(2), 32116.
76. Taucher, J., Arístegui, J., Bach, L.T., Guan, W., Montero, M.F., Nauendorf, A., Achterberg, E.P., Riebesell, U., 2018. Response of subtropical phytoplankton communities to ocean acidification under oligotrophic conditions and during nutrient fertilization. *Frontiers in Marine Science* 5, 330.
77. Thimijan, R. and Heins, R., 1983. Photometric, radiometric and quantum light units of measure: A review of procedures for interconversion. *Horticultural Science* 18: 818-822.
78. Tortell, P. D., DiTullio, G. R., Sigman, D. M., Morel, F. M., 2002. CO₂ effects on taxonomic composition and nutrient utilization in an Equatorial Pacific phytoplankton assemblage. *Marine Ecology Progress Series* 236, 37-43.
79. Tortell, P. D., Payne, C. D., Li Y., Trimborn, S., Rost, B., Smith, W. O., DiTullio, G. R., 2008. CO₂ sensitivity of Southern Ocean phytoplankton. *Geophysical Research Letters* 35(4).
80. Wells, M. L., Trainer, V. L., Smayda, T. J., Karlson, B. S., Trick, C. G., Kudela, R. M., and Cochlan, W. P., 2015. Harmful algal blooms and climate change: Learning from the past and present to forecast the future. *Harmful algae* 49, 68-93.

81. Xu, Y., Shi, D., Aristilde, L., & Morel, F. M. (2012). The effect of pH on the uptake of zinc and cadmium in marine phytoplankton: Possible role of weak complexes. *Limnology and oceanography*, 57(1), 293-304.
82. Young, J. N., Heureux, A. M., Sharwood, R. E., Rickaby, R. E., Morel, F. M., & Whitney, S. M. (2016). Large variation in the Rubisco kinetics of diatoms reveals diversity among their carbon-concentrating mechanisms. *Journal of Experimental Botany*, 67(11), 3445-3456.
83. Zhang, Y., Wang, T., Li, H., Bao, N., Hall-Spencer, J. M., Gao, K., 2018. Rising levels of temperature and CO₂ antagonistically affect phytoplankton primary productivity in the South China Sea. *Marine Environmental Research*, 141, 159-166.

Table 1: Initial and final values of carbon chemistry and dissolved inorganic nutrients under experimental conditions during Exp-I and II (values \pm SD; $n = 3$). Since we had used the same bulk seawater, the TA values were identical for both experiments. Please note that TA values presented here is the average of all initial and final samples ($n = 38$) from both experiments (there was no significant difference between the final and initial TA values). “ND” indicates not detectable. The concentrations of Zn and Cu in the natural water were $4.7 \pm 1.4 \text{ nM}$ and $11 \pm 3 \text{ nM}$, respectively.

		Parameters						
Exp-I (Zn)		PCO ₂ (μatm)	pH	TA ($\mu\text{mol kg}^{-1}$)	DIC ($\mu\text{mol kg}^{-1}$)	DIN ($\mu\text{mol kg}^{-1}$)	DIP ($\mu\text{mol kg}^{-1}$)	DSi ($\mu\text{mol kg}^{-1}$)
Initial	A-CO ₂	406 \pm 6	8.17 \pm 0.01	2250 \pm 15	1939 \pm 3	11.7 \pm 0.06	1.77 \pm 0.03	12.03 \pm 0.04
	H-CO ₂	943 \pm 166	7.87 \pm 0.07	2250 \pm 15	2093 \pm 28			
Final	A-CO ₂	178 \pm 20	8.40 \pm 0.04	2250 \pm 15	1791 \pm 29	0.43 \pm 0.39	0.14 \pm 0.02	4.69 \pm 0.21
	A-CO ₂ +Zn	182 \pm 14	8.39 \pm 0.03	2250 \pm 15	1797 \pm 19	2.36 \pm 1.73	0.06 \pm 0.02	1.69 \pm 0.32
	H-CO ₂	212 \pm 9	8.32 \pm 0.01	2250 \pm 15	1844 \pm 9.5	0.76 \pm 0.21	0.13 \pm 0.0	1.48 \pm 0.22
	H-CO ₂ +Zn	215 \pm 32	8.33 \pm 0.05	2250 \pm 15	1836 \pm 35	1.32 \pm 1.09	0.10 \pm 0.02	0.84 \pm 0.04
Exp-II (Cu)								
Initial	A-CO ₂	409 \pm 15	8.17 \pm 0.01	2250 \pm 15	1942 \pm 5.5	11.05 \pm 0.62	1.09 \pm 0.03	11.60 \pm 0.04
	H-CO ₂	998 \pm 17	7.84 \pm 0.007	2250 \pm 15	2106 \pm 2.7			
Final	A-CO ₂	255 \pm 16	8.33 \pm 0.02	2250 \pm 15	1839 \pm 15	0.073 \pm 0.04	ND	ND
	A-CO ₂ +1nM Cu	322 \pm 24	8.25 \pm 0.026	2250 \pm 15	1891 \pm 17	0.21 \pm 0.15	ND	0.89 \pm 0.06
	A-CO ₂ +2nM Cu	323 \pm 14	8.25 \pm 0.015	2250 \pm 15	1892 \pm 9.4	0.10 \pm 0.078	ND	0.72 \pm 0.09
	A-CO ₂ +8nM Cu	300 \pm 56	8.21 \pm 0.06	2250 \pm 15	1873 \pm 35	0.11 \pm 0.02	ND	0.79 \pm 0.07
	H-CO ₂	482 \pm 30	8.11 \pm 0.023	2250 \pm 15	1976 \pm 12	0.073 \pm 0.021	ND	1.94 \pm 0.19
	H-CO ₂ +1nM Cu	651 \pm 226	8.02 \pm 0.12	2250 \pm 15	2024 \pm 64	0.15 \pm 0.07	ND	1.38 \pm 0.5
	H-CO ₂ +2nM Cu	484 \pm 23	8.11 \pm 0.017	2250 \pm 15	1977 \pm 9.3	0.12 \pm 0.02	ND	0.91 \pm 0.25
	H-CO ₂ +8nM Cu	571 \pm 64	8.05 \pm 0.04	2250 \pm 15	2008 \pm 21	0.47 \pm 0.26	ND	0.79 \pm 0.26

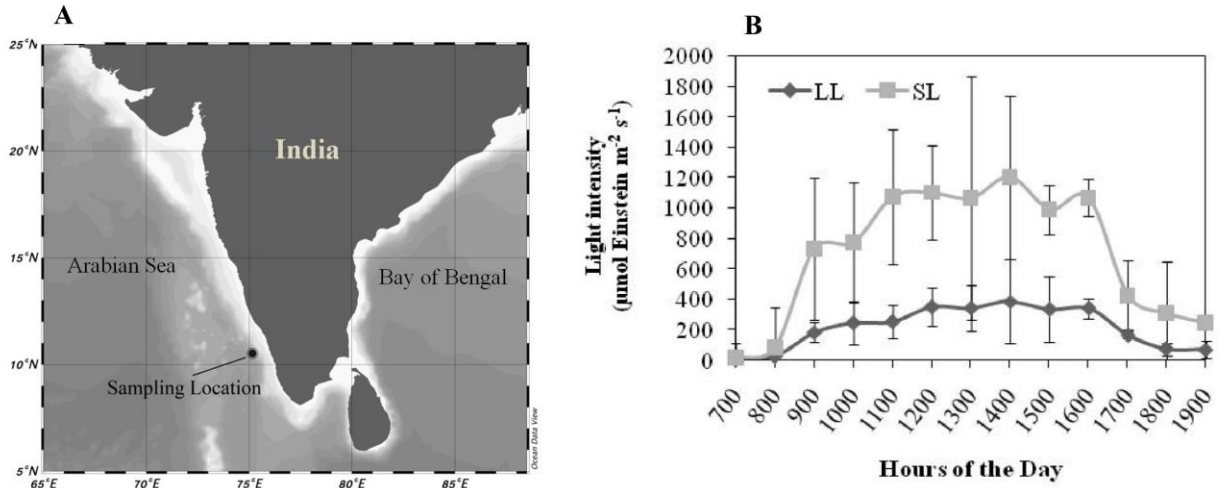


Fig.1: (A) Map showing the sampling location during August 2017 along the south west coast of India; (B) variability in solar light intensity during the experimental period; SL and LL represent surface light (100%) and low light intensity reaching at 2m depth, respectively (high variability was due to high frequent cloud coverage during the experimental)

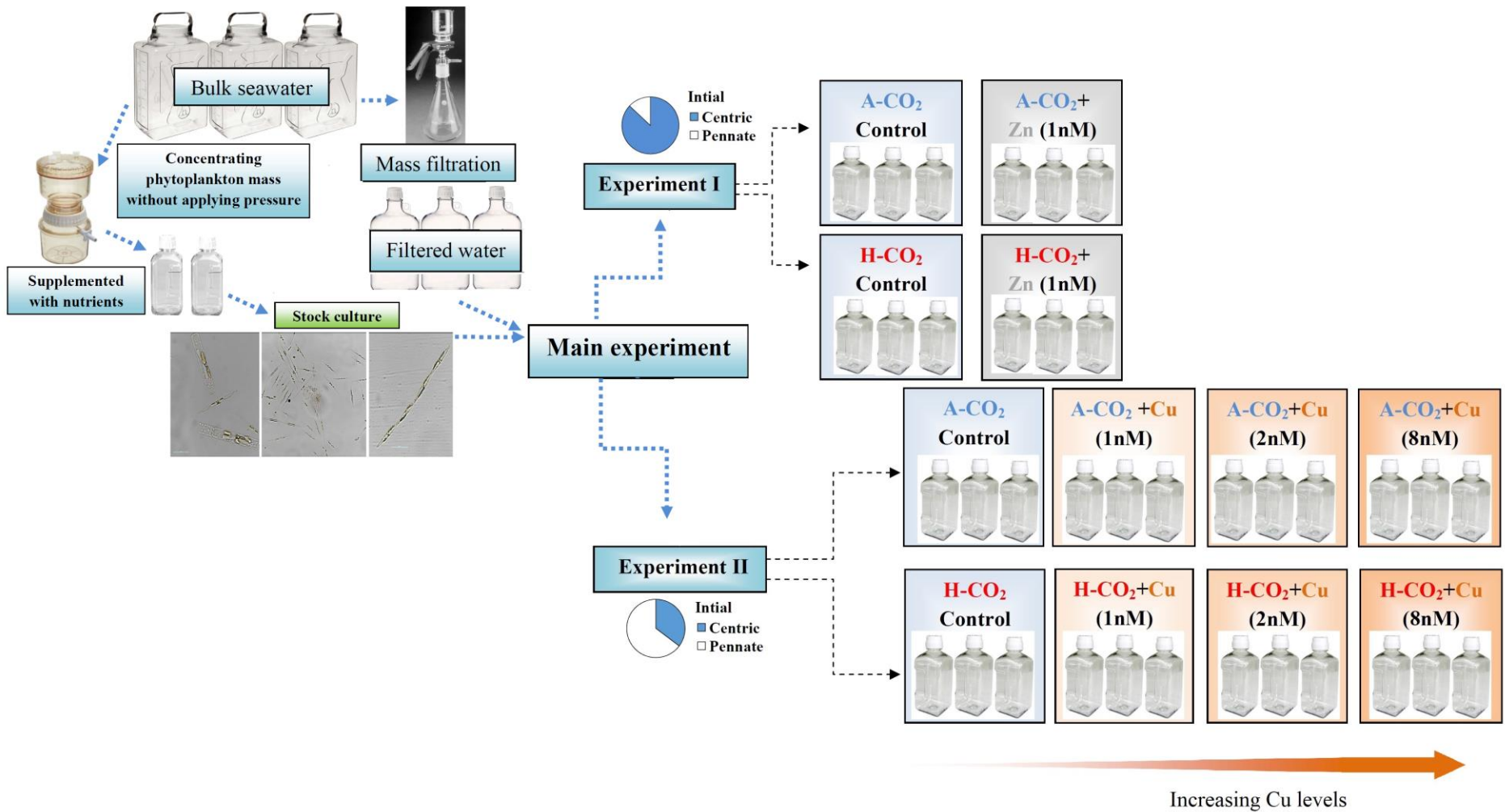


Fig. 2: Schematic representation of the experimental design showing the stock culture, different treatments with variable CO₂ (A-CO₂≈400μatm; H-CO₂≈1000μatm), Zn and Cu levels. Triplicate of each treatment is indicated as three bottles inside the box representing a particular treatment. Please note that there was a gap of 7 days between Exp-I to II and the initial phytoplankton community was significantly different as illustrated by the different relative contribution of pennate vs. centric diatoms.

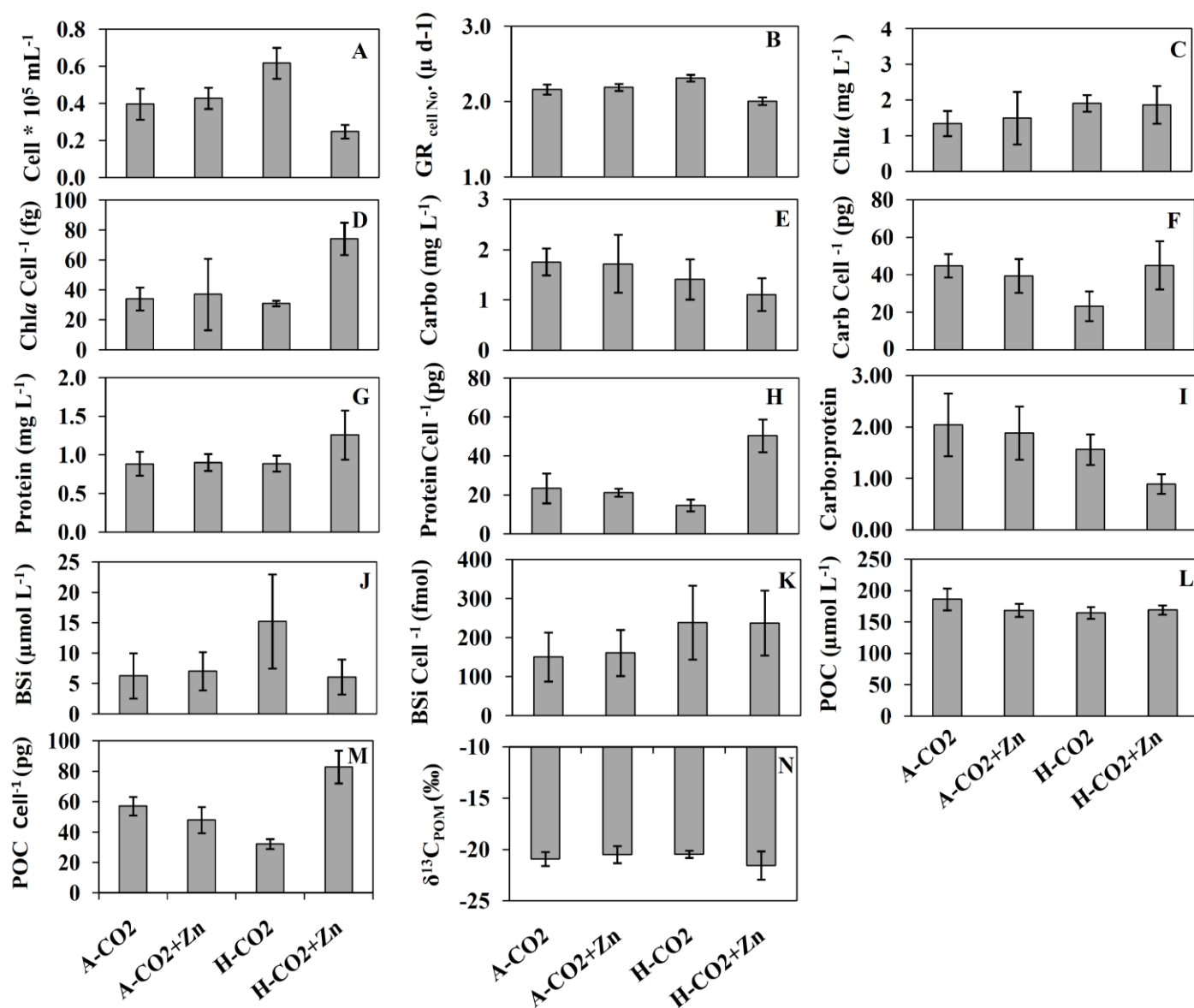


Fig. 3: Cell density (A); growth rate (B); Chla concentrations (C); Chla contents per cell (D); carbohydrate concentrations (E); carbohydrate contents per cell (F); protein concentrations (G); protein contents per cell (H); carbohydrate:protein ratio (I); BSi concentrations (J); BSi contents per cell (K); POC concentrations (L); POC content per cell (M) and $\delta^{13}\text{C}_{\text{POM}}$ values (N) under A-CO₂ ($\approx 400 \mu\text{atm}$) and H-CO₂ ($\approx 1000 \mu\text{atm}$) levels with Zn and without Zn addition (1nM) during Exp I.

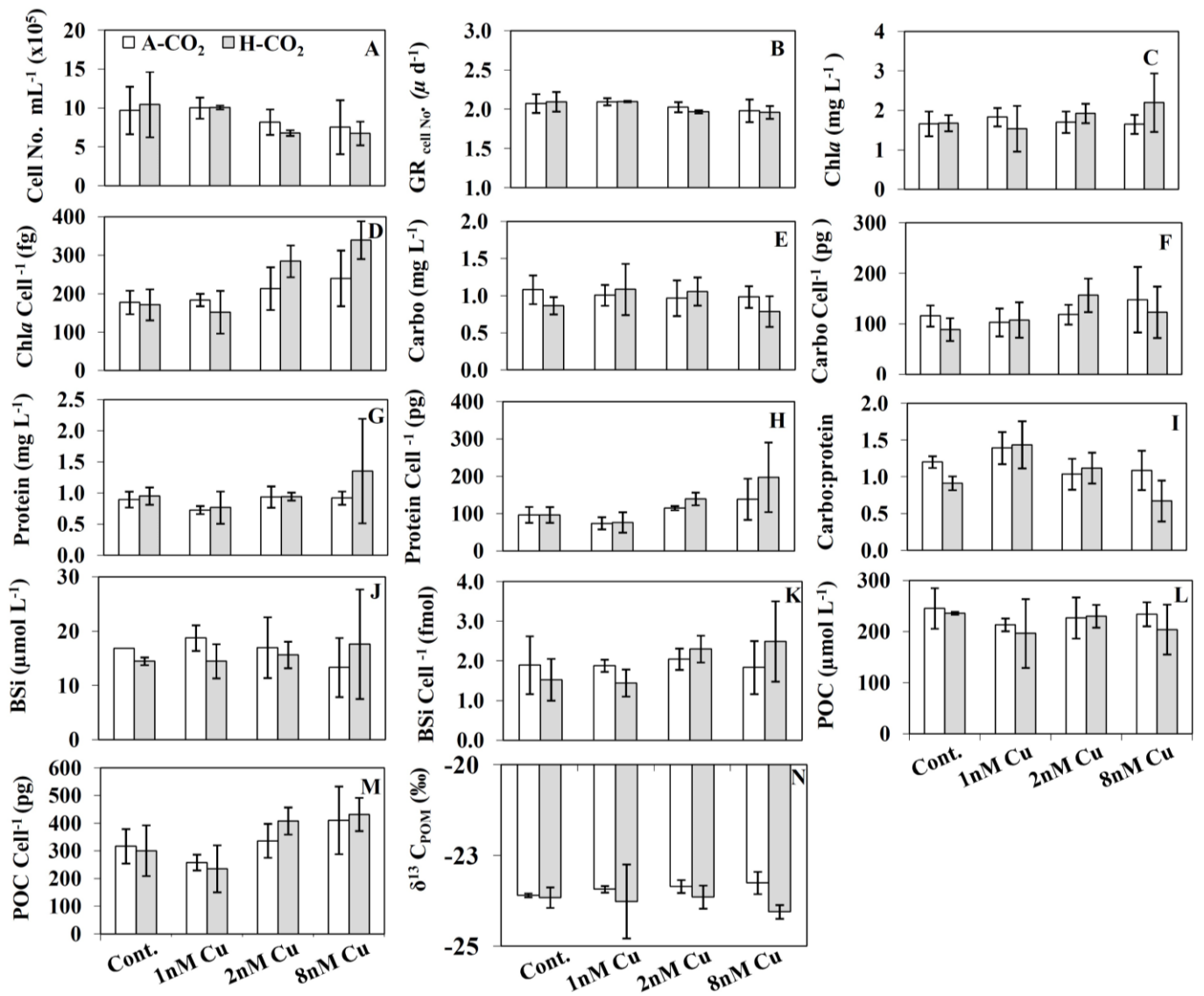


Fig. 4: Phytoplankton cell density (A); growth rate ($\mu_{\text{cell No.}} \cdot \text{d}^{-1}$) (B); Chla concentrations (C); per cell Chla contents (D); carbohydrate concentrations (E); per cell carbohydrate contents (F); protein concentrations (G); per cell protein contents (H) and the ratio of carbohydrate: protein (I); the concentrations of BSi (J); per cell BSi contents (K); the concentration of particulate organic carbon (POC) (L); per cell POC contents (M); and $\delta^{13}\text{C}_{\text{POM}}$ (‰) (N) under A-CO₂ ($\approx 400 \mu\text{atm}$) and H-CO₂ ($\approx 1000 \mu\text{atm}$) levels with variable Cu addition during Exp II.

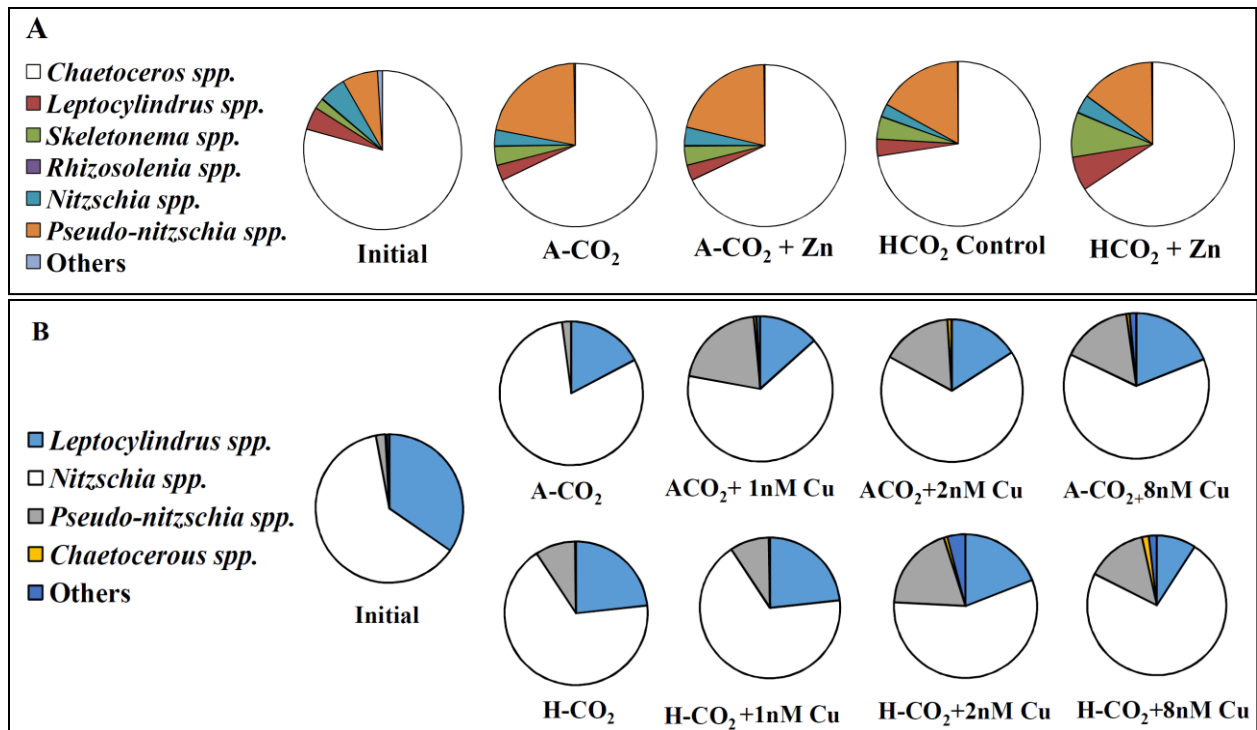


Fig. 5: Microscopic analysis of phytoplankton community composition [relative abundance (%)] in Exp I (A) and Exp-II (B).